

Published in final edited form as:

Nat Neurosci. ; 14(7): 874–880. doi:10.1038/nn.2835.

UNC119 is required for G protein trafficking in sensory neurons

Houbin Zhang^{1,*}, Ryan Constantine^{1,2,*}, Sergey Vorobiev³, Yang Chen³, Jayaraman Seetharaman³, Yuanpeng Janet Huang⁴, Rong Xiao⁴, Gaetano T. Montelione⁴, Cecilia D. Gerstner¹, M. Wayne Davis⁵, George Inana⁷, Frank G. Whitby⁸, Erik M. Jorgensen^{5,6}, Christopher P. Hill⁸, Liang Tong³, and Wolfgang Baehr^{1,5,9,#}

¹Department of Ophthalmology, University of Utah Health Science Center, Salt Lake City, UT 84132, USA

²Graduate Program in Neuroscience, University of Utah Health Science Center, Salt Lake City UT 84132, USA

³Department of Biological Sciences, Northeast Structural Genomics Consortium, Columbia University, New York, New York 10027, USA

⁴Center for Advanced Biotechnology and Medicine, Department of Molecular Biology and Biochemistry, Northeast Structural Genomics Consortium, Rutgers University, Piscataway, NJ 08854, USA

⁵Department of Biology, University of Utah, 257 South 1400 East, Salt Lake City, Utah 84112, USA

⁶Howard Hughes Medical Institute, University of Utah, 257 South 1400 East, Salt Lake City, Utah 84112, USA

⁷Bascom Palmer Eye Institute, University of Miami Miller School of Medicine, 1638 N.W., 10th Avenue, Miami, FL 33136, USA

⁸Department of Biochemistry, University of Utah School of Medicine, Salt Lake City, UT 84112-5650, USA

⁹Department of Neurobiology and Anatomy, University of Utah Health Science Center, Salt Lake City UT 84132, USA

SUMMARY

UNC119 is widely expressed among vertebrates and invertebrates. Here we report that UNC119 recognized the acylated N-terminus of the rod photoreceptor transducin α -subunit ($T\alpha$) as well as *C. elegans* G proteins Odr-3 and Gpa-13. The crystal structure of human UNC119 at 1.95 Å resolution revealed an immunoglobulin-like β -sandwich fold. Pulldowns and isothermal titration calorimetry revealed a tight interaction between UNC119 and acylated $G\alpha$ peptides. Co-

#Corresponding author: Wolfgang Baehr, Department of Ophthalmology, University of Utah Health Science Center, 65 N. Medical Dr, Salt Lake City, UT 84132 USA. Phone: 801-585-6643; fax: 801-585-1515; wbaehr@hsc.utah.edu.

*These authors contributed equally to this work

PROTEIN DATA BASE ACCESSION

UNC119: PDB 3GQQ

UNC119/lauroyl-GAGASAEKH: PDB 3RBQ

AUTHOR CONTRIBUTIONS

HZ generated pull-down/light-induced translocation results and is responsible for *C.elegans* immunostaining and imaging; RC generated ITC results; RC, FGW and CPH generated human UNC119/acylated $T\alpha$ -peptide co-crystals and solved the structure; SV, YC, JS, YJH, RX, GTM, and LT determined the human UNC119 structure; RC, CDG, and WB isolated ROS membranes, transducin and determined GTPase activity; MWD and EMJ generated transgenic *C. elegans* mutants; GI generated the Unc119 knockout mouse; HZ, RC, CPH, LT and WB wrote the manuscript;

crystallization of UNC119 with an acylated T α N-terminal peptide at 2.0 Å revealed that the lipid chain is buried deeply into UNC119's hydrophobic cavity. UNC119 bound T α ^{GTP} inhibiting its GTPase activity, thereby providing a stable UNC119-T α ^{GTP} complex that is capable of diffusing from the inner segment back to the outer segment following light-induced translocation. UNC119 deletion in both mouse and *C. elegans* lead to G protein mislocalization. These results establish UNC119 as a novel G α -subunit cofactor that is essential for G-protein trafficking in sensory cilia.

INTRODUCTION

Non-motile primary cilia sensitive to external stimuli are found in both vertebrate and invertebrate sensory neurons. In mammalian photoreceptors or *C. elegans* olfactory cells, light receptors (rhodopsin) or odorant receptors, together with their G-proteins and associated signal transduction components transport to cilia by vesicular and intraflagellar mechanisms. Defects in these trafficking pathways have been shown to impair signal transduction, ciliogenesis and cilia maintenance¹, often leading to severe disease. In both photoreceptors and odorant receptors, evidence shows that an ever increasing number of polypeptides is involved in vesicular trafficking and stabilizing intraflagellar transport, including components of the BBSome², Rab GTPases³, Arf- and Arf-like GTPases⁴ and prenyl binding proteins⁵.

UNC119 is 27 kDa polypeptide identified in the basal body proteome of *C. reinhardtii*⁶, the flagellar rootlet of *Naegleria*⁷, neurons of *C. elegans*⁸ and the mouse photoreceptor sensory cilium complex⁹. *unc-119* was first discovered in *C. elegans* on the basis of a spontaneous mutation affecting locomotion, feeding behavior and chemosensation⁸. Independently, a protein termed Retina Gene 4 (RG4) was discovered in the retina and recognized to be a *C. elegans unc-119* ortholog¹⁰. Although expressed in multiple tissues, UNC119 predominates in retinal photoreceptor inner segments and synaptic regions^{11–13}. UNC119 has been shown to interact with several diverse proteins, including the Arf-like GTPases ARL2¹⁴ and ARL3¹⁵, the Ca²⁺-binding protein CaBP4, a modulator of the voltage-gated Ca²⁺ channel Ca_v 1.4 present in rod and cone synapses¹⁶ and the synaptic ribbon component RIBEYE¹⁷ of photoreceptors. A heterozygous stop codon (K57ter) identified in the human *UNC119* gene of a patient with late-onset dominant cone dystrophy also produced dominant dystrophy in a transgenic mouse model¹⁸.

Apart from the mammalian retina, UNC119 has been detected in leukocytes (eosinophils), T-cells, lung fibroblasts¹⁹, the adrenal glands, cerebellum and kidney¹¹. UNC119 has also been shown to activate Src-type tyrosine kinases associated with the interleukin-5 receptor and the T-cell receptor by interacting with Src homology domains located in the N-terminal half of UNC119²⁰. Widespread distribution of UNC119 in vertebrates, invertebrates and even flagellated protozoa suggests highly conserved and multiple functions throughout the animal kingdom.

Here we identify UNC119 as a novel lipid binding protein interacting with acylated N-termini of G-protein α subunits present in mouse photoreceptors and *C. elegans* olfactory neurons. The crystal structure at 1.95 Å resolution reveals that UNC119 adopts an immunoglobulin-like β -sandwich fold. The N-terminal peptide of transducin- α (T α) inserts deeply into the hydrophobic cavity formed by the β -sandwich fold of UNC119. Remarkably, the ligand enters the protein interior from the opposite side of that seen for structurally related proteins and the first six amino acid residues of the T α peptide are deeply buried in the core making intimate contacts with UNC119. UNC119 knockouts demonstrate the requirement of UNC119 for G protein trafficking in animal models as diverse as mouse and *C. elegans*.

RESULTS

The structure of human UNC119 at 1.95Å resolution

The crystal structure of human UNC119 (residues 57–237) at 1.95 Å resolution (PDB ID 3GQQ) contains an immunoglobulin-like β -sandwich fold comprised of two β -sheets (Figs. 1A,B). The β -sheets, arranged in four antiparallel strands fold in a Greek key pattern (Fig. S1A), which is found in a large number of diverse proteins²¹. Strands β 3– β 4 and β 7– β 8 are linked by short α -helical loops (α 1 and α 2 in Fig. 1A). In the UNC119 structure, the two sheets are splayed apart from each other at one edge of this β -sandwich, revealing a narrow, deep cavity penetrating the center of this structure (Fig. 1A). The atomic model is in agreement with the crystallographic data and expected stereochemistry (Table S1).

A search of the Protein Data Bank with the program DaliLite (<http://www.ebi.ac.uk/Tools/dalilite/index.html>) returned a large number of similar structures including PrBP/ δ (Z score 12, 24% overall amino acid sequence identity with UNC119), and Rho-GDP dissociation inhibitor 1 (RhoGDI, Z score 9, 10% overall identity) (Fig. S1B, S2A). When restricted to the region that folds into β -sheets, UNC119 sequence similarity with PrBP/ δ increased to 56% (Fig. S1C). PrBP/ δ is a prenyl-binding protein that interacts with prenylated proteins participating in phototransduction⁵, while RhoGDI regulates the function of the Rho GTPase CDC42²². Both proteins possess a hydrophobic pocket capable of accommodating farnesyl and geranylgeranyl chains^{23, 24}. The aforementioned structural similarities suggested that UNC119 might be a lipid binding protein.

UNC119 interacts with the transducin α -subunit

To identify interacting partners of UNC119 in photoreceptors, we used the GST fusion protein pulldown technique followed by HPLC and tandem mass spectrometry (LC-MS/MS). From bovine retina lysates, we identified a polypeptide of approximately 40 kDa that specifically bound GST-UNC119 (asterisk, Fig. 2A). Sequence identification by LC-MS/MS yielded numerous peptides matching the rod $T\alpha$ -subunit, and one matching cone $T\alpha$ (Fig. 2B), both of which are involved in phototransduction. In the inactive state GDP is bound to $T\alpha$, permitting the interaction with $T\beta\gamma$, yielding the heterotrimeric complex, $T\alpha\beta\gamma$. To test whether UNC119 pulled down the heterotrimeric complex through its interaction with $T\alpha$, pulldowns were repeated using wild-type and *Gnat1*^{-/-} ($T\alpha$ knockout) mouse retina lysates (Fig. 2C). Immunoblots probed with anti- $T\alpha$ and anti- $T\gamma$ antibodies showed that UNC119 interacts with $T\alpha$, but not with farnesylated $T\gamma$ (Fig. 2C, lane 4). Pulldowns were negative using *Gnat1*^{-/-} retina lysates (Fig. 2C, lanes 7,8) confirming that UNC119 is not a prenyl binding protein.

The glycine residue at the N-terminus of rod $T\alpha$ (G2) is heterogeneously acylated²⁵ carrying either C12:0, C14:1, C14:2, or C14:0 side chains, which play an important role in targeting $T\alpha$ to the outer segment²⁶. Due to the structural similarity among UNC119, PrBP/ δ , and RhoGDI, we suspected that UNC119 would interact with the N-terminal acyl group of $T\alpha$. To test this hypothesis, G2 at the N-terminus of $T\alpha$ was replaced with alanine, a mutation preventing $T\alpha$ acylation. Recombinant $T\alpha$ (G2A) did not interact with bovine GST-UNC119 in pulldown assays (Fig. 2D, lane 5) suggesting that the acyl side chain attached to G2 of $T\alpha$ mediates the interaction with GST-UNC119. Furthermore, UNC119 failed to interact with N-myristoylated GCAP1 (Fig. 2E, lower panel) or recoverin (not shown), suggesting that the interaction with UNC119 requires some degree of specificity.

UNC119 is an acyl-binding protein

To independently confirm that UNC119 is a novel acyl-binding protein, a synthetic lauroylated (C12:0) peptide corresponding to the N-terminus of bovine T α (2-GAGASAEK-11) was added to the pulldown assay. The acylated T α peptide was able to competitively inhibit binding of T α to UNC119 (Fig. 3A, lane 3), whereas the unacylated peptide had no effect (Fig. 3A, lane 4). These results support the requirement for the N-terminal acyl group as a mediator of the interaction between T α and UNC119.

We then employed isothermal titration calorimetry (ITC) to determine the binding constant of acylated N-terminal G protein α -subunit peptides with UNC119 (Fig. 3B). ITC measures the binding enthalpy of two reactants enabling the resolution of two or more binding sites. We titrated the acylated N-terminal bovine T α peptides and the acylated N-terminal *C. elegans* ODR-3 peptide (GSCQSNENSE). ODR-3 is expressed in *C. elegans* AWA, AWB, and AWC olfactory neurons and participates in chemosensory signal transduction (the *unc-119* null mutation was originally discovered in *C. elegans*)⁸. Microcalorimetry experiments showed that the unacylated T α peptide does not interact with recombinant human UNC119, whereas lauroyl- and myristoyl-GAGASAEK each exhibited tight binding at a single site with K_D s of approximately $0.54 \mu\text{M} \pm 0.28 \mu\text{M}$ and $0.22 \mu\text{M} \pm 0.14 \mu\text{M}$, respectively (Fig. 3B). This dissociation constant is similar to those measured *in vitro* for farnesyl and geranylgeranyl side chains with PrBP/ δ ($0.7 \mu\text{M}$, and $19 \mu\text{M}$, respectively)²⁴. UNC119 also bound the lauroylated N-terminal peptide derived from ODR-3, but did so by two orders of magnitude weaker than the lauroyl T α peptide ($K_D = 16.4 \mu\text{M} \pm 3.0 \mu\text{M}$), further implicating the N-terminal residues in binding specificity. Alignment of mouse N-terminal G α peptides revealed that the *Gna11-15* and *Gnaq* subfamilies are not N-terminally acylated (Fig. 3C) indicating that the UNC119-G α subunit interaction does not extend to all G α subfamilies.

The UNC119 hydrophobic cavity is the lipid binding site

Interpretation of our structural and biochemical results suggested that the lipid inserts into the hydrophobic cavity at the center of the β -sandwich. The co-crystal structure of UNC119 with the lauroylated T α peptide at 2.0 \AA (PDB ID: 3RBQ) showed that the pocket easily accommodates a lauroyl (C12) moiety (Fig. 4) in a very specific fashion as each molecule in the asymmetric unit of the crystal contains a similarly bound ligand (Table S2 and Fig. S3). The cavity is lined predominantly by hydrophobic residues (mostly Phe and Tyr) that mediate the interaction with the lauroylated T α peptide primarily via *Van der Waals* forces, consistent with properties of a lipid binding site (Fig. 4C, S2C). Remarkably, entrances to the lipid binding sites of PrBP/ δ and RhoGDI (Fig. S1B) do not exist in UNC119, but instead are found on the opposite edge of the β -sandwich (Figs. 4A,B, S2A,B).

The lauroyl group and the first six residues of the T α peptide are buried deeply within the hydrophobic pocket of UNC119 (Figs. 4C, S2C), whereas peptide residues 7–10 make only peripheral contact with UNC119 and are poorly ordered. In general, the surrounding protein residues formed a surface that is highly complementary to the shape of the ligand, thereby rationalizing the high degree of conservation for the N-terminal residues of T α and the contacting residues of UNC119. As expected for a hydrophobic environment, hydrogen bonding potentials were satisfied by specific interactions. The first six peptide residues lack polar side chains, with the exception of S6, which sits exposed to solvent. Most of the main chain groups participate in hydrogen bonds through the formation of a distorted 3_{10} - α helix by the first six residues of the peptide. Remaining buried polar groups of the peptide are coordinated by conserved UNC119 residues. The Y131 hydroxyl group hydrogen bonds with the lauroyl oxygen, E163 hydrogen bonds G2 NH, and Y220 coordinates A3 NH via a buried water molecule (Fig. 4C). This water molecule, along with E163 and Y220, constitute

part of an extensive hydrogen-bonding network that also includes H165, H192, Y194, S218, and one other water molecule. These interactions provide specific recognition of N-terminal groups that define the location of the peptide-acyl junction within the UNC119 cavity, thereby establishing the length of acyl chain that can be accommodated. We have also determined an isomorphous structure of UNC119 with the *C. elegans* ODR-3 lauroyl-GSCQSNENSE ligand (data not shown). This structure is superimposable with that of the $T\alpha$ ligand but with a less-ordered peptide structure, consistent with the weaker binding affinity and absence of amino acid residues relevant for optimal binding.

Transducin-membrane interactions are regulated by GTP and UNC119

The co-crystal structure of UNC119 with the acylated $T\alpha$ peptide implies that UNC119 may disrupt membrane association of $T\alpha$ by inserting the acyl chain into its hydrophobic pocket. To investigate whether UNC119 facilitates dissociation of transducin from membranes under isotonic conditions where it is firmly membrane associated, we examined the extraction of $T\alpha$ by UNC119 in the presence and absence of GTP. $T\alpha$ could be extracted from rod outer segments (ROS) membranes by UNC119 only in the presence of GTP (Fig. 5A), suggesting that GTP/GDP exchange and disruption of $T\alpha T\beta\gamma$ are essential for dissociation.

To demonstrate that UNC119 does not extract $T\alpha^{GDP}T\beta\gamma$ from membranes, we investigated the interaction of UNC119 with $T\alpha^{GTP}$ and $T\alpha^{GDP}T\beta\gamma$. *In vitro*, association of $T\alpha^{GDP}T\beta\gamma$ to membranes can be disrupted in the dark by low salt (hypotonic) buffers in the absence of GTP²⁷. In contrast, in the light, transducin is tightly bound to rhodopsin, requiring GDP/GTP exchange for disruption of the complex and membrane dissociation. $T\alpha^{GTP}$ and $T\alpha^{GDP}T\beta\gamma$ containing retinal lysates were prepared from light-adapted and dark-adapted retina, respectively, and used for pulldown assays. Pulldowns indicated that UNC119 formed stable complexes only with $T\alpha^{GTP}$ (Fig. 5B, left panel), but not with $T\alpha^{GDP}T\beta\gamma$ (Fig. 5B, right panel), confirming that disruption of $T\alpha$ from $T\alpha^{GDP}T\beta\gamma$ is necessary for the formation of the UNC119- $T\alpha^{GTP}$ complex.

To determine whether UNC119 binding to $T\alpha^{GTP}$ inhibits the GTPase activity of $T\alpha$, we measured GTP hydrolysis in a reconstituted system. Depleted ROS membranes containing rhodopsin exhibited very low GTPase activity originating from the remaining traces of transducin in the ROS membranes (Fig. 5C). The addition of transducin reconstituted GTPase activity yielding a K_{cat} of 1.5 moles $GTP_{hydrolyzed}/mol$ transducin/min. However, $T\alpha$ -GTPase activity was nearly completely inhibited in the presence of recombinant UNC119. Collectively, these results show that neither GTP nor UNC119 alone, was effective in solubilizing $T\alpha$ from light-adapted membranes. The ability of UNC119 to extract $T\alpha^{GTP}$ from membranes and stabilize GTP suggests that UNC119 may play a key role in the light-induced translocation of transducin (see discussion).

UNC119 deletion in mouse affects transducin trafficking in photoreceptors

The *Unc119*^{-/-} mouse shows no obvious retinal degeneration early in life, but develops a slowly progressing photoreceptor degeneration beginning 6 months postnatally¹². In the dark-adapted *Unc119*^{-/-} retina, $T\alpha$ is partially retained in the inner segment and outer nuclear layer (Fig. 6B), while in the dark-adapted wild-type retina, $T\alpha$ is detected almost exclusively in the outer segment (Fig. 6A). Transducin is thought to arrive at the outer segment by either vesicular transport²⁸ or passive diffusion²⁹, and UNC119 deletion appeared to have no effect on its localization.

A fascinating property of transducin is its observed translocation to the inner segment in bulk during intense light exposure as part of a light-adaptation and desensitization

mechanism. Under intense light, $T\alpha^{GTP}$ and $T\beta$ translocate individually to the inner segment within minutes^{30, 31} by diffusion³². Both $T\alpha$ and $T\beta$ return to the outer segments in hours during prolonged dark-adaptation³⁰, presumably by restricted diffusion²⁹, as transducin does return to outer segments in eyecups depleted of ATP, which is required for molecular motor-driven transport. To determine the effect of UNC119 deletion on the return of transducin by diffusion, we exposed wild-type and *Unc119*^{-/-} mice to intense light for 60 min followed by prolonged dark-adaptation (0–24 hours) (Fig. 6C–K). Return of $T\alpha$ was nearly complete in wild-type photoreceptors after three hours of dark-adaptation, yet a significant amount of $T\alpha$ remained associated with *Unc119*^{-/-} inner segment membranes following prolonged dark-adaptation (Fig. 6F,H,J). The partial efficacy of UNC119 deletion on $T\alpha$ mislocalization and the resulting slow degeneration may be attributable to redundant UNC119 isoforms (see discussion).

Trafficking of ODR-3 and GPA-13 in *C. elegans* olfactory neurons requires UNC119

Originally discovered in *C. elegans*, *unc-119* mutants exhibit a complex phenotype, including defects in chemosensation, altered feeding behavior, inability to form dauer larvae⁸ and excessive branching of motor neuron commissures³³. We suspected G-protein participation in polypeptide trafficking to olfactory cilia and investigated the consequences of the *unc-119* deletion in *C. elegans* olfactory neurons. Although several G proteins participate in chemosensory signal transduction, ODR-3, predicted to be acylated at G2, is required to mediate signal transduction in AWA and AWC sensory neurons³⁴. ODR-3 is localized predominantly to the cilia, with only trace amounts found in the dendrites and cell bodies³⁵. Immunolabeling of wild-type (Figs. 7A, S4A) and *unc-119* mutant worms (Figs. 7B, S4B) with antibody directed against ODR-3 revealed mislocalization of ODR-3 in the *unc-119* mutant worms. Correspondingly, while GPA-13 was present in the cilia of both wild-type (Figs. 7C, S4C) and *unc-119* mutant (Figs. 7D, S4D) ADF, ASH and AWC chemosensory neurons³⁵, it was down-regulated and mislocalized in the mutant worm.

Reduced amounts of ODR-3 and GPA-13 present in the cilia of mutant worms could arise indirectly from abnormal neuronal morphology. To exclude this possibility, transgenic worms specifically expressing GFP in AWA, AWB or AWC neurons were crossed onto the *unc-119* mutant background. Ciliated endings of AWA and AWB neurons in *unc-119* mutants (Fig. S4F,H) were identical to wild-type (Fig. S4E,G), but the shape of the AWC sensory ending in *unc-119* mutants (Fig. S4J) was slightly different from wild-type (Fig. S4I). As the ciliary morphology of AWC neurons in the *unc-119* mutant was normal, however, it seems improbable that the decreased ODR-3 and GPA-13 protein levels observed in *unc-119* mutants were caused by disrupted cellular integrity.

To determine whether expression of transgenic, wild-type *unc-119* could restore G protein stability in amphid neurons, GFP::UNC-119 driven by the *gpa-13* promoter was introduced into *unc-119* mutant worms. GFP::UNC-119 expression was found in three pairs of amphid sensory neurons--presumably ADF, ASH and AWC (Fig. 7E,G). Labeling with anti-GPA-13 antibody showed an increase in GPA-13 immunoreactivity in the cilia of the transgenic worms (Fig. 7E) relative to nontransgenic *unc-119* mutants (Fig. 7F). Because ODR-3 is also expressed in ADF, ASH and AWC neurons, transgenic worms were also labeled with anti-ODR-3 antibody. Increased levels of ODR-3 were also detected in the cilia of transgenic worms (Fig. 7G) relative to nontransgenic *unc-119* mutant worms (Fig. 7H). Transgenic expression of supplemental UNC-119 in these neurons was capable of restoring the wild-type phenotype.

DISCUSSION

The immunoglobulin β -sandwich fold demonstrated by the crystal structure of human UNC119 is similar to that seen in PrBP/ δ (PDB ID:1KSH)²³ and RhoGDI (PDB ID:1DOA)²². PrBP/ δ is a prenyl binding protein and an important cofactor in the transport of prenylated proteins in photoreceptors⁵. RhoGDI extracts C-terminally geranylgeranylated Rac, Rho, and CDC42 from membranes providing a hydrophobic environment for their prenyl anchors in its pocket, thereby trapping these small G proteins in their inactive GDP bound form²². The β -strands of PrBP/ δ and UNC119 align nicely when the two structures are superimposed (Fig. S2A), while the β -strands of RhoGDI and UNC119 are more divergent (Fig. S2B). Important differences are seen in the UNC119 structure. The entrance through which the lipid enters the hydrophobic pocket in RhoGDI (and presumably PrBP/ δ) is located at the opposite edge of the β -sandwich fold. The opening of the UNC119 pocket is completely occupied by the first six amino acids of T α with the acyl chain deeply inserted into the cavity. These data, along with the extensive interactions that limit the depth to which the T α peptide can penetrate the UNC119 cavity (Figs. 4C,S2A,B), support the assertion that interaction specificity with lipidated proteins is based in part upon the amino acid sequence immediately adjacent to the posttranslational modification.

Unc119 and G protein trafficking

G-protein subunits are either co-translationally acylated or acylated by an unidentified ER-resident acyl transferase. Acylated G α and prenylated G $\beta\gamma$ most likely combine to form heterotrimeric G proteins at the ER²⁸. Our results (Fig. 6B) show that the deletion of UNC119 in mouse leads to partial retention of transducin in the inner segment even after complete dark-adaptation, leaving post-biosynthesis transport largely intact. The partial effect seen in the *UNC119*^{-/-} mouse is likely due to the redundancy of UNC119 isoforms. UNC119B, encoded by the *UNC119B* gene located on human chromosome 5 (*UNC119* is on chromosome 17) is 61% similar and 52% identical to UNC119 and like GST-UNC119, GST-UNC119B pulls down T α from bovine retina lysate (RC and WB, unpublished results).

In contrast to vertebrates, the *C. elegans* genome harbors only one UNC119 gene. Accordingly, *unc-119* null mutant phenotypes are more severe and UNC-119 deletion affects both neuronal and non-neuronal cells resulting in a complex phenotype. We focused on olfactory neurons as defects in chemosensation have been reported in *unc-119* worms⁸. *C. elegans* relies on its 11 pairs of amphid neurons to detect odorants and soluble molecules³⁶. These sensory neurons are polarized ciliated cells with an overall morphology similar to vertebrate photoreceptors. *unc-119* deletion in the worm results in the mislocalization and mistargeting of the G proteins ODR-3 and GPA-13, which are expressed in AWA, AWB, and AWC as well as in ASH and ADF amphid cells (Fig. 7B,D). Proper localization of ODR-3 and GPA-13 was restored by expressing transgenic UNC119 under the control of their intrinsic promoters (Fig. 7E,G). Interestingly, ODR-3, GPA-13 and T α share only 27% overall sequence identity, with sequence similarity at the N-terminal 50 amino acids being very limited. The ODR-3 N-terminal peptide shares only three of ten amino acids with the T α peptide (Fig. 3C), resulting in a lower affinity interaction with human UNC119 as shown by isothermal titration calorimetry (Fig. 3B).

Light-induced translocation of transducin by diffusion

Light-activation of rhodopsin triggers GTP/GDP exchange on T α causing T α ^{GTP} and T $\beta\gamma$ to dissociate and traffic to the inner segment by passive diffusion with a $t_{1/2}$ of 3–5 min for T α and a $t_{1/2}$ of approximately 12 min for T $\beta\gamma$ ³². T $\beta\gamma$ is known to associate with phosducin, which reduces its affinity for both T α and rod outer segment membranes³⁷. Upon return to the dark, both T α and T $\beta\gamma$ subunits return to the outer segments in hours in wild-type mice.

This same phenomenon has previously been described in eyecups depleted of ATP, without which, molecular motors do not function²⁹. Therefore, a model in which "restricted" diffusion is responsible for the return of $T\alpha$ and $T\beta\gamma$ to the outer segments is plausible.

We propose that the restriction is provided by an enzymatically switchable sink in the inner segments. We determined that UNC119 elutes $T\alpha$ bound to membranes only in the presence of GTP (Fig. 5B), suggesting that the dissociation of $T\alpha^{GTP}$ and $T\beta\gamma$ is essential for UNC119/ $T\alpha^{GTP}$ complex formation. Upon arrival at the inner segment following light-induced translocation (Fig. S5A), transducin subunits are presumed to recombine after $T\alpha$'s intrinsic GTPase activity hydrolyzes GTP, permitting heterotrimeric transducin to dock to inner segment membranes which are devoid of rhodopsin. In the absence of the guanine exchange factor rhodopsin (Fig. S5B), GTP/GDP exchange is very slow (rate constant 10^{-4} /sec)³⁸. Both the GTP requirement for $T\alpha$ extraction from membranes and the slow rate constant suggest that this event is the rate-limiting step for return to the outer segment (Fig. S5B). The rate constant dictates that it will take approximately 10^4 seconds (166 minutes) for transducin to return to the outer segment, which agrees with experimentally observed return rates^{31, 32}. Upon solubilization of the UNC119/ $T\alpha$ -GTP complex, it likely diffuses passively through the inner segment and connecting cilium, depositing $T\alpha$ directly at discs in the outer segment. Following $T\alpha^{GTP}$ solubilization, PrBP/ δ may extract $T\beta\gamma$, whose transport to the outer segment is severely affected in a PrBP/ δ deletion model⁵. An alternate candidate for interaction with $T\beta\gamma$ is phosducin, deletion of which affects light-driven translocation of $T\beta\gamma$ to the inner segment³⁷. The detection of UNC119 in the mouse photoreceptor sensory cilium complex⁹ suggests a possible role for UNC119 in cargo assembly and IFT, an argument that is further strengthened by the association of UNC119 with ARL3 and RP2 (retinitis pigmentosa protein 2), both of which localize to mouse and human cilia^{9, 15}.

Our data provide evidence for UNC119 functioning as a novel lipid binding protein as well as a necessary component in G protein trafficking. UNC119, along with G proteins, is distributed in virtually all living organisms from unicellular flagellated amoeba to mammals. Thus, our data in both mouse and *C. elegans* will likely prove helpful in elucidating mechanisms involved in membrane protein transport in the sensory systems of other species.

Supplementary Material

Refer to Web version on PubMed Central for supplementary material.

Acknowledgments

We thank Randy Abramowitz and John Schwanof for access to the X4A beamline at NSLS; G. DeTitta of Hauptman Woodward Research Institute for crystallization screening. This work was supported by National Institute of Health grants EY08123 (WB), EY019298 (WB), EY014800-039003 (NEI core grant), EY10848 (GI), by the Howard Hughes Medical Institute (EJ) and by NIH Grant NS034307 (EJ), by a grant from the Protein Structure Initiative of the National Institutes of Health (U54 GM074958), by the University of Utah Macromolecule Crystallography Core Facility, by a Center Grant of the Foundation Fighting Blindness, Inc., (Columbia MD), to the University of Utah, and unrestricted grants to the Departments of Ophthalmology at the University of Utah from Research to Prevent Blindness (New York, N.Y.). WB is a recipient of a Research to Prevent Blindness Senior Investigator Award.

Reference List

1. Rosenbaum JL, Witman GB. Intraflagellar transport. *Nat. Rev. Mol. Cell Biol.* 2002; 3:813–825. [PubMed: 12415299]
2. Jin H, et al. The conserved Bardet-Biedl syndrome proteins assemble a coat that traffics membrane proteins to cilia. *Cell.* 2010; 141:1208–1219. [PubMed: 20603001]

3. Kim J, Krishnaswami SR, Gleeson JG. CEP290 interacts with the centriolar satellite component PCM-1 and is required for Rab8 localization to the primary cilium. *Hum. Mol. Genet.* 2008; 17:3796–3805. [PubMed: 18772192]
4. Gillingham AK, Munro S. The small G proteins of the Arf family and their regulators. *Annu. Rev. Cell Dev. Biol.* 2007; 23:579–611. [PubMed: 17506703]
5. Zhang H, et al. Deletion of PrBP/{delta} impedes transport of GRK1 and PDE6 catalytic subunits to photoreceptor outer segments. *Proc. Natl. Acad. Sci U. S. A.* 2007; 104:8857–8862. [PubMed: 17496142]
6. Keller LC, et al. Molecular architecture of the centriole proteome: the conserved WD40 domain protein POC1 is required for centriole duplication and length control. *Mol. Biol. Cell.* 2009; 20:1150–1166. [PubMed: 19109428]
7. Chung S, Kang S, Paik S, Lee J. NgUNC-119, Naegleria homologue of UNC-119, localizes to the flagellar rootlet. *Gene.* 2007; 389:45–51. [PubMed: 17123749]
8. Maduro M, Pilgrim D. Identification and cloning of unc-119, a gene expressed in the *Caenorhabditis elegans* nervous system. *Genetics.* 1995; 141:977–988. [PubMed: 8582641]
9. Liu Q, et al. The proteome of the mouse photoreceptor sensory cilium complex. *Mol. Cell Proteomics.* 2007; 6:1299–1317. [PubMed: 17494944]
10. Higashide T, Murakami A, McLaren MJ, Inana G. Cloning of the cDNA for a novel photoreceptor protein. *J. Biol. Chem.* 1996; 271:1797–1804. [PubMed: 8576185]
11. Swanson DA, Chang JT, Campochiaro PA, Zack DJ, Valle D. Mammalian orthologs of *C. elegans* unc-119 highly expressed in photoreceptors. *Invest. Ophthalmol. Vis. Sci.* 1998; 39:2085–2094. [PubMed: 9761287]
12. Ishiba Y, et al. Targeted inactivation of synaptic HRG4 (UNC119) causes dysfunction in the distal photoreceptor and slow retinal degeneration, revealing a new function. *Exp Eye Research.* 2007; 84:473–485.
13. Higashide T, McLaren MJ, Inana G. Localization of HRG4, a photoreceptor protein homologous to Unc-119, in ribbon synapse. *Invest Ophthalmol. Vis. Sci.* 1998; 39:690–698. [PubMed: 9538874]
14. Kobayashi A, Kubota S, Mori N, McLaren MJ, Inana G. Photoreceptor synaptic protein HRG4 (UNC119) interacts with ARL2 via a putative conserved domain. *FEBS Lett.* 2003; 534:26–32. [PubMed: 12527357]
15. Veltel S, Kravchenko A, Ismail S, Wittinghofer A. Specificity of Arl2/Arl3 signaling is mediated by a ternary Arl3-effector-GAP complex. *FEBS Lett.* 2008; 582:2501–2507. [PubMed: 18588884]
16. Haeseleer F. Interaction and Colocalization of CaBP4 and Unc119 (MRG4) in Photoreceptors. *Invest Ophthalmol. Vis. Sci.* 2008; 49:2366–2375. [PubMed: 18296658]
17. Alpadi K, et al. RIBEYE recruits Munc119, a mammalian ortholog of the *Caenorhabditis elegans* protein unc119, to synaptic ribbons of photoreceptor synapses. *J Biol. Chem.* 2008; 283:26461–26467. [PubMed: 18664567]
18. Kobayashi A, et al. HRG4 (UNC119) mutation found in cone-rod dystrophy causes retinal degeneration in a transgenic model. *Invest Ophthalmol. Vis. Sci.* 2000; 41:3268–3277. [PubMed: 11006213]
19. Vepachedu R, Karim Z, Patel O, Goplen N, Alam R. Unc119 protects from *Shigella* infection by inhibiting the Abl family kinases. *PLoS. ONE.* 2009; 4:e5211. [PubMed: 19381274]
20. Gorska MM, Cen O, Liang Q, Stafford SJ, Alam R. Differential regulation of interleukin 5-stimulated signaling pathways by dynamin. *J Biol. Chem.* 2006; 281:14429–14439. [PubMed: 16556602]
21. Bork P, Holm L, Sander C. The immunoglobulin fold. Structural classification, sequence patterns and common core. *J. Mol. Biol.* 1994; 242:309–320. [PubMed: 7932691]
22. Hoffman GR, Nassar N, Cerione RA. Structure of the Rho family GTP-binding protein Cdc42 in complex with the multifunctional regulator RhoGDI. *Cell.* 2000; 100:345–356. [PubMed: 10676816]
23. Hanzal-Bayer M, Renault L, Roversi P, Wittinghofer A, Hillig RC. The complex of Arl2-GTP and PDE delta: from structure to function. *EMBO J.* 2002; 21:2095–2106. [PubMed: 11980706]
24. Zhang H, et al. Photoreceptor cGMP phosphodiesterase delta subunit (PDEdelta) functions as a prenyl-binding protein. *J. Biol. Chem.* 2004; 279:407–413. [PubMed: 14561760]

25. Goc A, et al. Different properties of the native and reconstituted heterotrimeric G protein transducin. *Biochemistry*. 2008; 47:12409–12419. [PubMed: 18975915]
26. Kerov V, et al. N-terminal fatty acylation of transducin profoundly influences its localization and the kinetics of photoresponse in rods. *J Neurosci*. 2007; 27:10270–10277. [PubMed: 17881533]
27. Baehr W, Morita E, Swanson R, Applebury ML. Characterization of bovine rod outer segment G protein. *J. Biol. Chem*. 1982; 257:6452–6460. [PubMed: 7076677]
28. Marrari Y, Crouthamel M, Irannejad R, Wedegaertner PB. Assembly and trafficking of heterotrimeric G proteins. *Biochemistry*. 2007; 46:7665–7677. [PubMed: 17559193]
29. Slepak VZ, Hurley JB. Mechanism of light-induced translocation of arrestin and transducin in photoreceptors: interaction-restricted diffusion. *IUBMB. Life*. 2008; 60:2–9. [PubMed: 18379987]
30. Sokolov M, et al. Massive light-driven translocation of transducin between the two major compartments of rod cells: a novel mechanism of light adaptation. *Neuron*. 2002; 34:95–106. [PubMed: 11931744]
31. Elias RV, Sezate SS, Cao W, McGinnis JF. Temporal kinetics of the light/dark translocation and compartmentation of arrestin and alpha-transducin in mouse photoreceptor cells. *Mol. Vis*. 2004; 10:672–681. [PubMed: 15467522]
32. Calvert PD, Strissel KJ, Schiesser WE, Pugh EN Jr, Arshavsky VY. Light-driven translocation of signaling proteins in vertebrate photoreceptors. *Trends Cell Biol*. 2006; 16:560–568. [PubMed: 16996267]
33. Knobel KM, Davis WS, Jorgensen EM, Bastiani MJ. UNC-119 suppresses axon branching in *C. elegans*. *Development*. 2001; 128:4079–4092. [PubMed: 11641230]
34. Roayaie K, Crump JG, Sagasti A, Bargmann CI. The G alpha protein ODR-3 mediates olfactory and nociceptive function and controls cilium morphogenesis in *C. elegans* olfactory neurons. *Neuron*. 1998; 20:55–67. [PubMed: 9459442]
35. Lans H, Rademakers S, Jansen G. A network of stimulatory and inhibitory Galpha-subunits regulates olfaction in *Caenorhabditis elegans*. *Genetics*. 2004; 167:1677–1687. [PubMed: 15342507]
36. Perkins LA, Hedgecock EM, Thomson JN, Culotti JG. Mutant sensory cilia in the nematode *Caenorhabditis elegans*. *Dev. Biol*. 1986; 117:456–487. [PubMed: 2428682]
37. Sokolov M, et al. Phosducin facilitates light-driven transducin translocation in rod photoreceptors. Evidence from the phosducin knockout mouse. *J Biol. Chem*. 2004; 279:19149–19156. [PubMed: 14973130]
38. Cowan CW, Wensel TG, Arshavsky VY. Enzymology of GTPase acceleration in phototransduction. *Methods Enzymol*. 2000; 315:524–538. [PubMed: 10736724]
39. Troemel ER, Kimmel BE, Bargmann CI. Reprogramming chemotaxis responses: sensory neurons define olfactory preferences in *C. elegans*. *Cell*. 1997; 91:161–169. [PubMed: 9346234]
40. Acton TB, et al. Robotic cloning and Protein Production Platform of the Northeast Structural Genomics Consortium. *Methods Enzymol*. 2005; 394:210–243. [PubMed: 15808222]
41. Chayen NE, Stewart PD, Maeder DL, Blow DM. An automated system for micro-batch protein crystallization and screening. *J. Appl. Cryst*. 1990; 23:297–302.
42. Otwinowski Z, Minor D. Processing of X-ray diffraction data collected in oscillation mode. *Meth. Enzymol*. 1997; 276:307–326.
43. Schneider TR, Sheldrick GM. Substructure solution with SHELXD. *Acta Crystallogr. D. Biol. Crystallogr*. 2002; 58:1772–1779. [PubMed: 12351820]
44. Terwilliger TC. SOLVE and RESOLVE: automated structure solution and density modification. *Methods Enzymol*. 2003; 374:22–37. [PubMed: 14696367]
45. Emsley P, Cowtan K. Coot: model-building tools for molecular graphics. *Acta Crystallogr. D. Biol. Crystallogr*. 2004; 60:2126–2132. [PubMed: 15572765]
46. Adams PD, et al. PHENIX: building new software for automated crystallographic structure determination. *Acta Crystallogr. D. Biol. Crystallogr*. 2002; 58:1948–1954. [PubMed: 12393927]
47. Davis IW, et al. MolProbity: all-atom contacts and structure validation for proteins and nucleic acids. *Nucleic Acids Res*. 2007; 35:W375–W383. [PubMed: 17452350]

48. McCoy AJ, et al. Phaser crystallographic software. *J. Appl. Crystallogr.* 2007; 40:658–674. [PubMed: 19461840]
49. Jones TA, Zou JY, Cowan SW, Kjeldgaard M. Improved methods for building protein models in electron density maps and the location of errors in these models. *Acta Crystallogr. A.* 1991; 47(Pt 2):110–119. [PubMed: 2025413]
50. Murshudov GN, Vagin AA, Dodson EJ. Refinement of macromolecular structures by the maximum-likelihood method. *Acta Crystallogr. D. Biol. Crystallogr.* 1997; 53:240–255. [PubMed: 15299926]

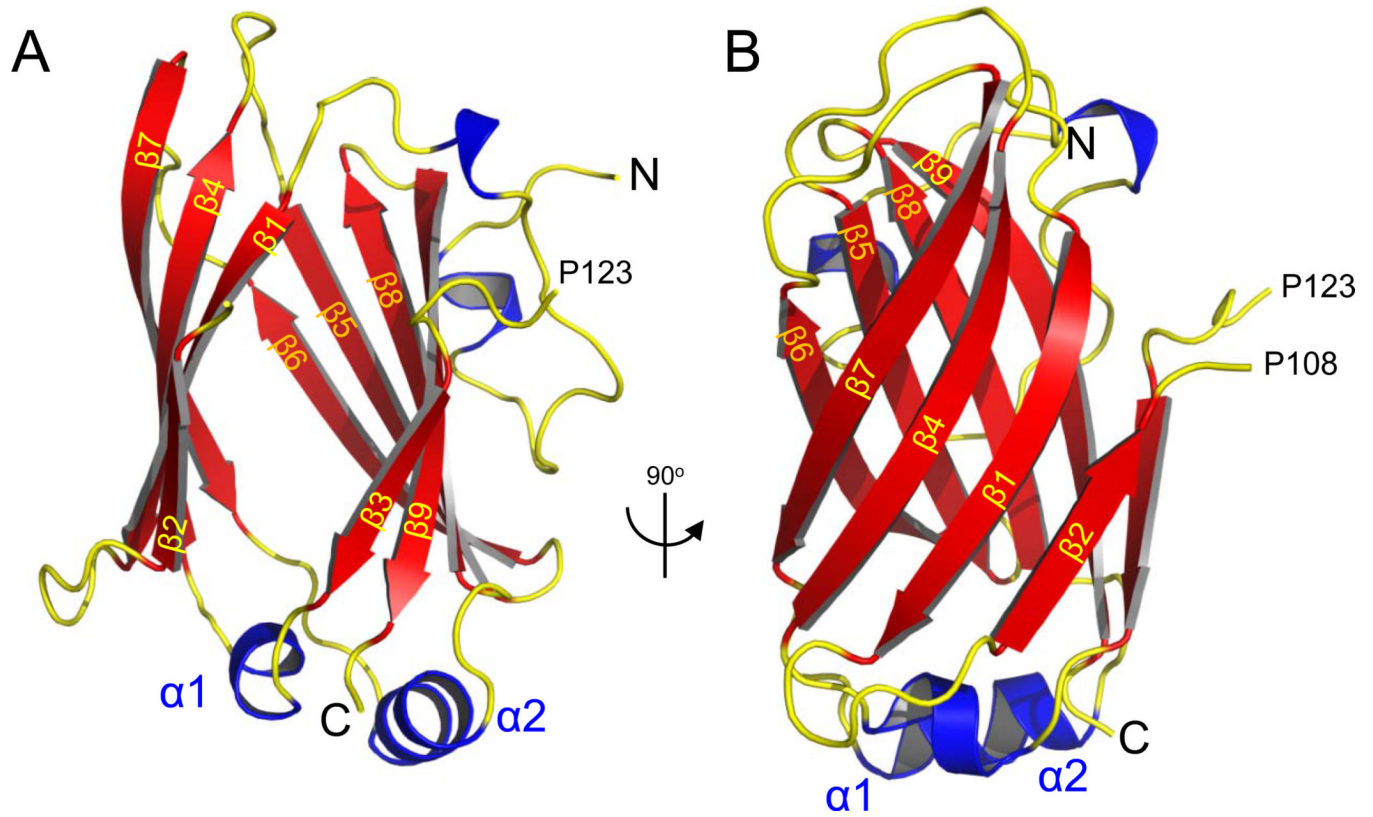


Figure 1. Crystal structure of human UNC119

(A) Ribbon representation of the structure of human UNC119 (residues 57–237). Nine β strands (β 1– β 9), shown in red, create two β -sheets that splay apart at one end to create an opening to the cavity at the center of the β -sandwich. The N- and C-termini are marked N and C, respectively. The structure of the loop 108–123 connecting strands β 2 and β 3 could not be resolved. (B) Structure of UNC119 viewed after a 90° rotation around the vertical axis.

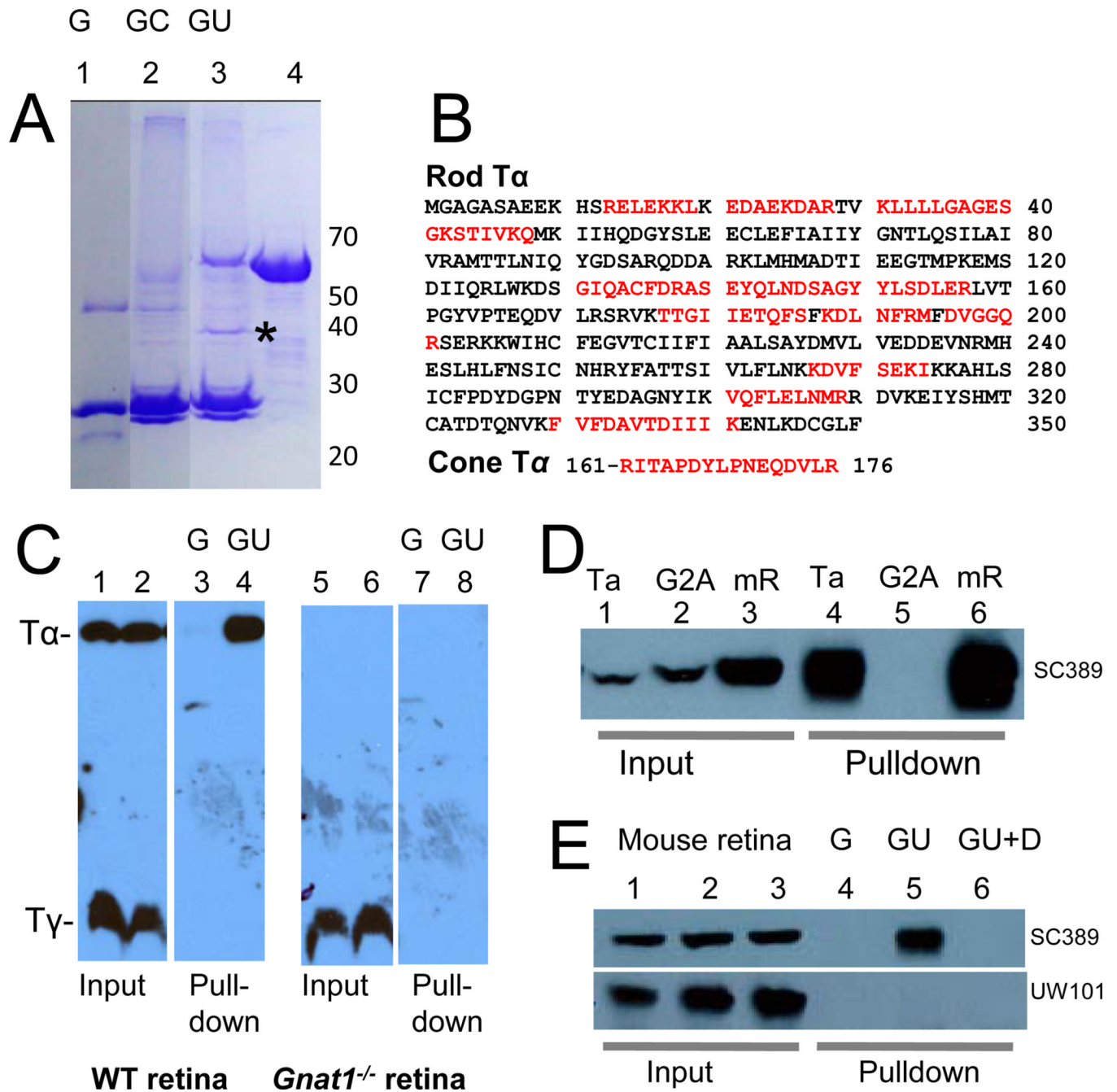


Figure 2. Interaction of UNC119 with Tα polypeptides

(A) Pull-down of rod and cone Tα with GST-UNC119 (representative Coomassie stained gel of four independent experiments). Bound polypeptides from bovine retina lysates were analyzed by SDS-PAGE. Lane 1, recombinant GST (G); Lane 2, pull-down with GST as a control (GC); Lane 3, GST-UNC119 pull-down (GU); Lane 4, GST-UNC119 fusion protein. An asterisk identifies the proteins pulled down by GST-UNC119. (B) Identification of peptides by LC-MS/MS. The 40 kDa polypeptides pulled down with GST-UNC119 were sequenced by LC-MS/MS. Identified peptide sequences, shown in red, were matched with rod and cone Tα. (C) GST-UNC119 pull-down of Tα from wild-type (lanes 1–4) and *Gnat1*^{-/-} retina (lanes 5–8). Lanes 1,2,5,6, input; lanes 3,7, control pull-downs with GST;

lanes 4,8, pulldowns with GST-UNC119. Acylated T α is pulled down (lane 4), but not farnesylated T γ (lane 8). **(D)** GST-UNC119 pulldown of T α and T α (G2A) expressed in HEK cells. Lanes 1–3, input; lanes 4–6, pulldowns. Lanes 1,4, HEK cells expressing bovine T α ; Lanes 2,5, HEK cells expressing bovine T α (G2A); Lanes 3 and 6, mouse retina lysates. Blot was probed with anti-T α antibody. Note that UNC119 does not interact with non-acylated T α (G2A). **(E)** Specificity of retina lysate pulldowns. Lanes 1–3, mouse retina lysates (input); lanes 4–6, retina lysate pulldowns; lane 4, GST control; lane 5, 10 μ g GST-UNC119 was added; lane 6, same as lane 5 but with 0.1% Triton X-100 and 0.1% NP-40 (DT) present in the binding buffer. Top panel, blot probed with anti-T α . Bottom panel, same blot probed with anti-GCAP1 antibody. Note that myristoylated GCAP1 does not interact with GST-UNC119.

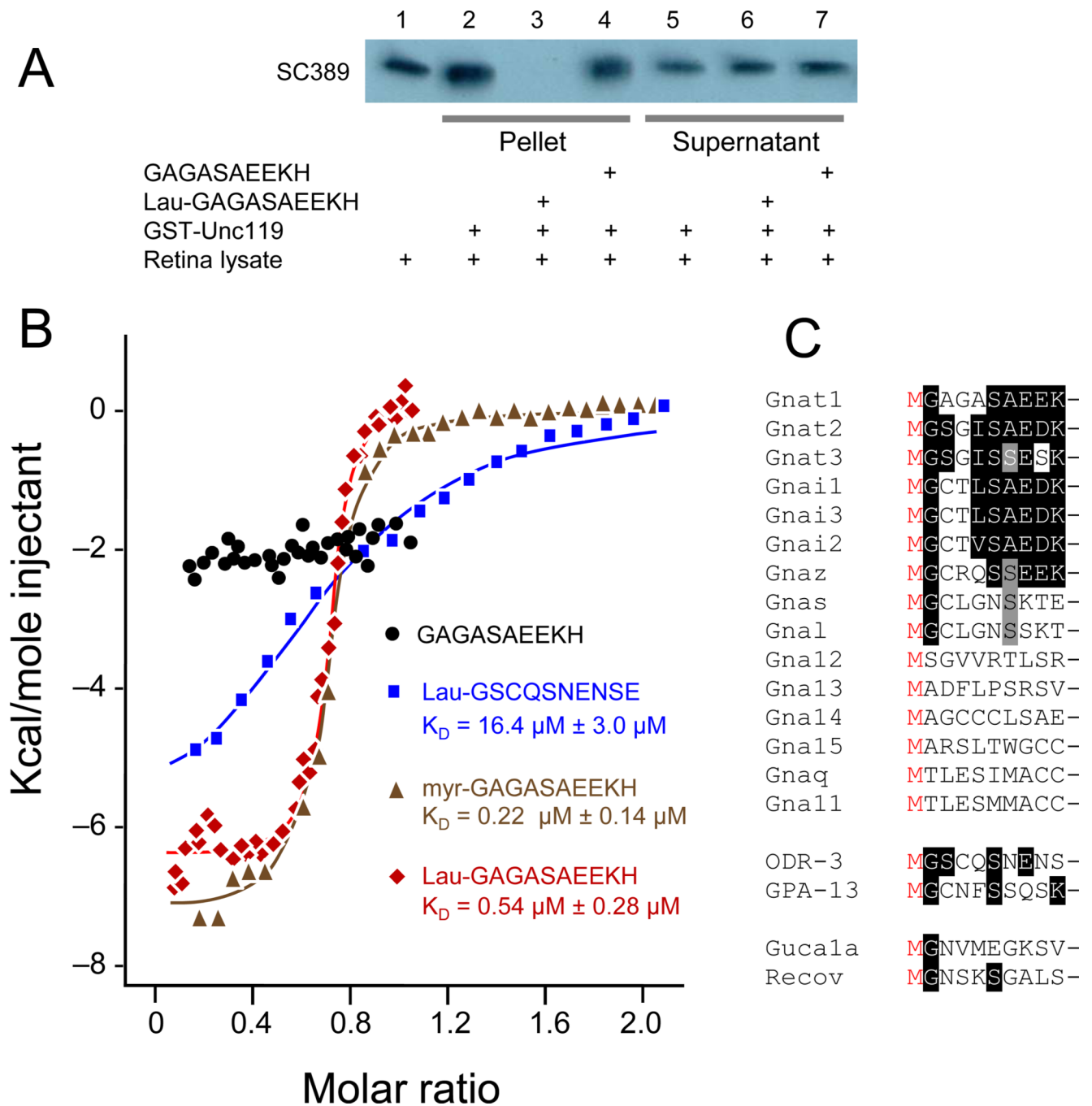


Figure 3. UNC119 is an acyl-binding protein

(A) GST-UNC119 pull-downs and inhibition by an acylated N-terminal α peptide. Lane 1, retina lysate. Lanes 2–4, glutathione bead pellets of retina lysates that were incubated with GST-UNC119, in the absence of peptide (lane 2), the presence of lauroyl-GAGASAEKHK (lane 3), and in the presence of non-acylated GAGASAEKHK peptide (lane 4). Lanes 5–7, supernatants of 2–4. Note that lauroyl-GAGASAEKHK competes for binding (lane 3), but the non-acylated peptide did not (lane 4). (B) Isothermal titration calorimetry. Human UNC119 was titrated with G protein α -subunit N-terminal peptides. Red symbols, titration with N-terminal α peptide (lauroyl-GAGASAEKHK); black circles, titration with non-lauroylated GAGASAEKHK; green triangles, titration with myristoylated GAGASAEKHK;

blue squares, titration with ODR-3 N-terminal peptide lauroyl-GSCQSNENSE. Lauroyl-GAGASAEKHK (red) and myristoyl-GAGASAEKHK (green) peptides were fit to a one-site model and bind with K_{DS} of $0.54 \mu\text{M} \pm 0.28 \mu\text{M}$ and $0.22 \mu\text{M} \pm 0.14 \mu\text{M}$, respectively. Lauroyl-ODR-3 (blue) binds more than one order of magnitude weaker ($16.4 \mu\text{M} \pm 3.0 \mu\text{M}$). (C) Alignment of N-terminal peptides of mouse G protein α subunits, *C. elegans* G protein α -subunits GPA-13 and ODR-3, and Ca^{2+} -binding proteins GCAP1, GCAP2 and recoverin. Peptides lacking Gly at position 2 cannot be myristoylated, therefore interaction with UNC119 through an acyl chain does not extend to all subfamilies of $G\alpha$.

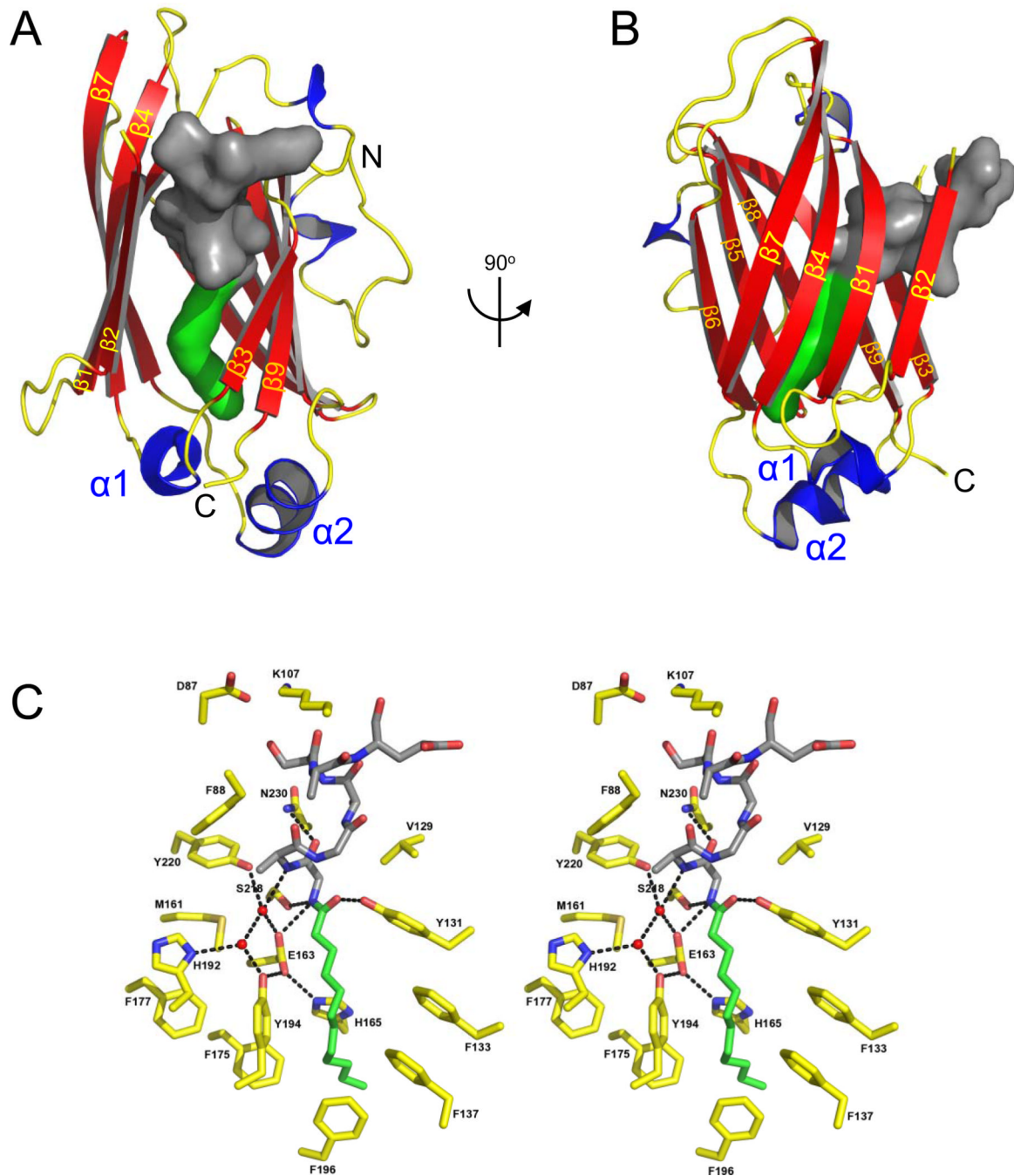


Figure 4. The lipid binding pocket of UNC119

(A,B) Two orientations of UNC119 co-crystallized with the acylated T α peptide in the UNC119 hydrophobic cavity. The lauroyl chain is shown in green, and the ten amino acids of the peptide are modeled in dark gray. In B, UNC119 is viewed after a 90° rotation around the vertical axis and the individual β -strands are labeled β 1-9 in yellow. (C) Stereoview of UNC119 residues and key water molecules interacting with the lauroyl-GAGASAEKHK ligand. The hydrogen-bonding network (black dashed lines) limits the depth to which the T α peptide can penetrate UNC119. Hydrogen bonds were included if the average of the bond length for all six molecules in the asymmetric unit was 3.2 Å or less and satisfied appropriate hydrogen bonding stereochemistry. UNC119 residues are shown in yellow, the

lauroyl chain is green and the attached residues are colored dark gray. Figures were created with PyMOL (www.pymol.org).

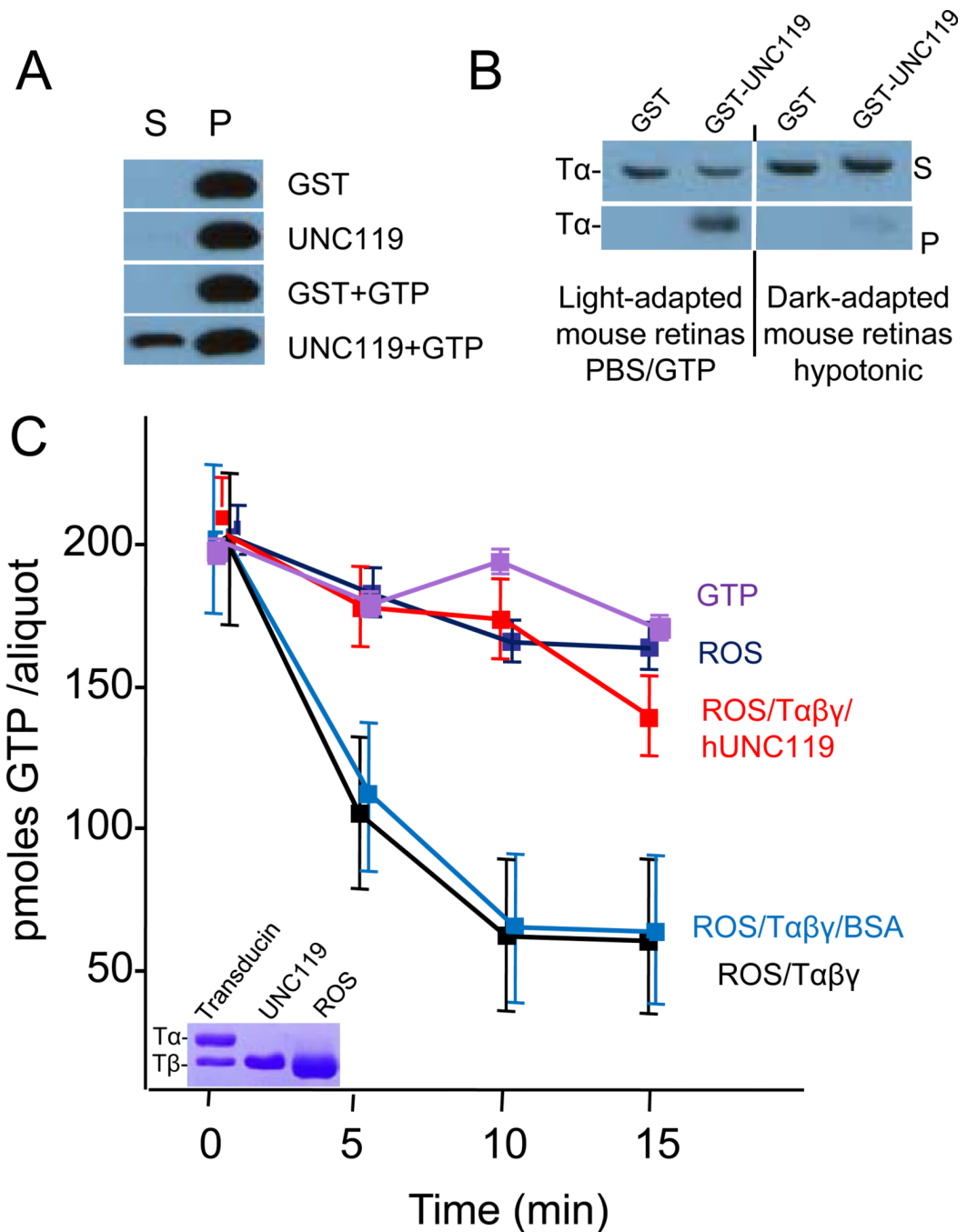


Figure 5. UNC119 Interacts with T α -GTP and Inhibits GTPase Activity

(A) Extraction of T α from membranes by UNC119. Live mice were exposed to 10,000 lux/20 minutes driving transducin to the inner segments. Retina lysates in 1X PBS were incubated with either GST, mUNC119, GST and GTP, or mUNC119 and GTP, respectively. The soluble proteins (S) were separated from membrane-bound proteins (P) by centrifugation. T α was detected by western blot using anti-T α antibody. T α elutes only in the presence of UNC119 and GTP. (B) Pull-down assays with light-adapted and dark-adapted mouse retinas. PBS/GTP supernatants from retinas of a light-adapted mouse (2,000 lux) and hypotonic supernatants from retinas of a dark-adapted mouse were used for pull-down assays, respectively. The proteins pulled down by GST or GST-UNC119 (pellet) and

unbound proteins (supernatant) were analyzed by western blot using anti-T α antibody. GST-UNC119 binds T α ^{GTP} (left), but not T α ^{GDP}T β γ (right). (C) GTPase activity of purified T α β γ in the presence of ROS membranes. The activity of the reconstituted system (red line) corresponds to a rate of 1.5 mole GTP/min. Addition of BSA (light blue) has little effect, whereas addition of UNC119 (green) reduces the activity nearly to baseline. Baseline activity is caused by a low amount of T α β γ still attached to the membranes (see inset). Inset, SDS-PAGE of purified native transducin (only T α and T β subunits are shown), recombinant human UNC119 and depleted ROS membranes containing rhodopsin and a trace of transducin (only T α is visible, T β co-migrates with rhodopsin).

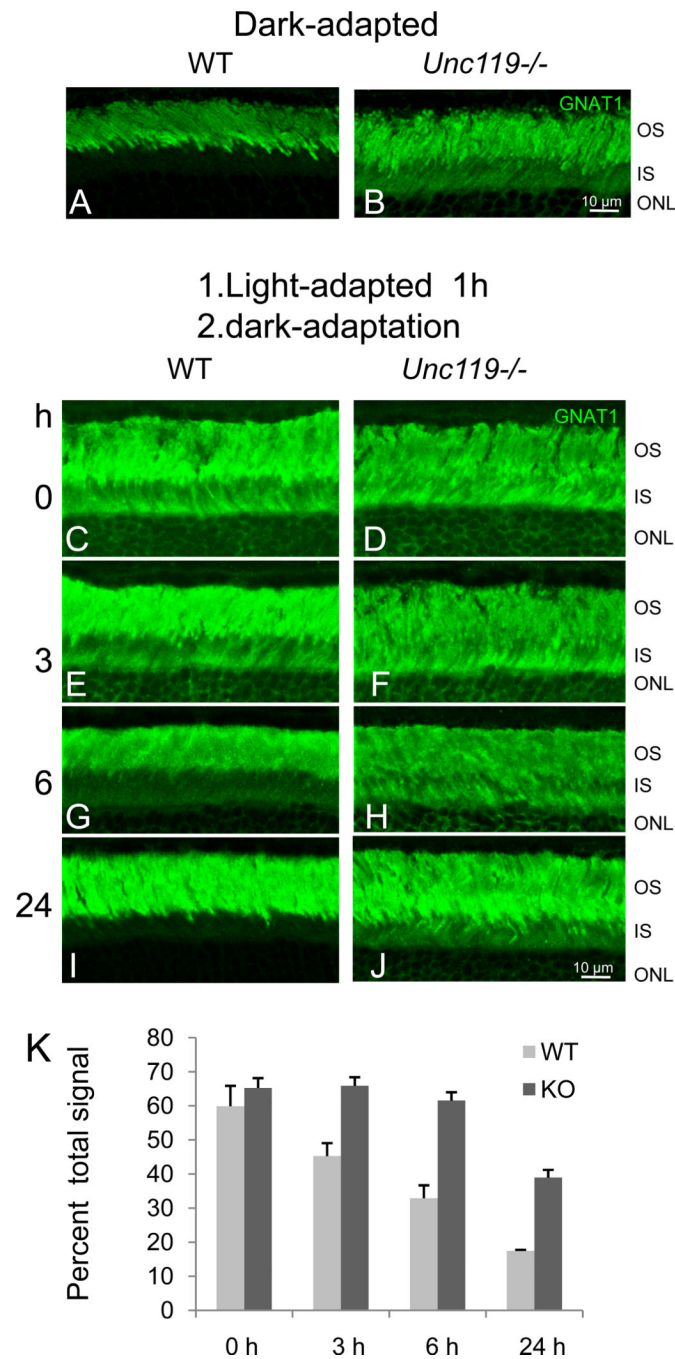


Figure 6. Slow Return of Transducin to the Outer Segment after Intense Light Exposure
(A,B) Localization of $T\alpha$ (green) in dark-adapted wild-type and *Unc119*^{-/-} retina. Mice were dark-adapted for at least 12 hours. Frozen sections were probed with anti- $T\alpha$ antibody and FITC-linked secondary antibody. Note the presence of $T\alpha$ in dark-adapted inner segments. **(C–J)** Mice were first exposed to intense light for 60 minutes, then dark-adapted for 0–24 hours. Frozen sections were probed with anti- $T\alpha$ and FITC-linked secondary antibody. Note that $T\alpha$ slowly returns to the wild-type outer segment, but is blocked in part from returning to the *Unc119*^{-/-} outer segment. OS, outer segment; IS, inner segment; ONL, outer nuclear layer. **(K)** Quantification of inner segment fluorescence at 0, 3, 6, and 24 hours after start of dark-adaptation. Fluorescence signal was quantified using ImageJ

software. Each bar included three independent measurements. Error bars denote means \pm SD.

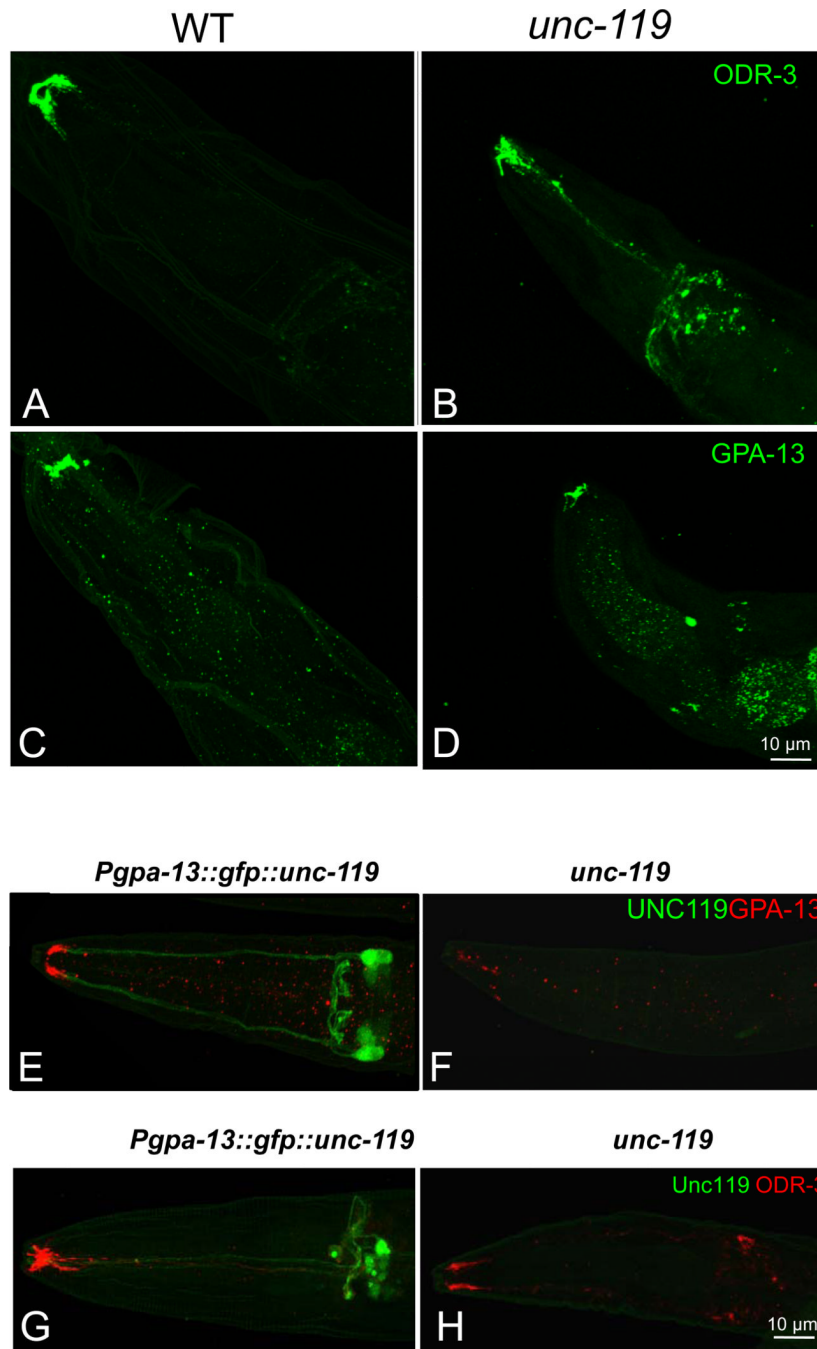


Figure 7. Mislocalization of the G proteins ODR-3 and GPA-13 in a *C. elegans unc-119(ed3)* mutant

(A–D) Wild-type (A,C) and *unc-119* mutant (B,D) *C. elegans* were stained with an anti-ODR-3 (A,B) and anti GPA-13 (C,D) antibody. Mislocalization of ODR-3 and GPA-13 to the olfactory cell bodies and axons is evident in *unc-119* mutants. (E–H) Cell-specific rescue of *unc-119* in *C. elegans* restores GPA-13 and ODR-3 localization. The *unc-119* gene fused with GFP was driven by the *gpa-13* promoter in ADF, ASH and AWC in *unc-119* mutants. The transgenic (E,G) and *unc-119* mutant control (F,H) were labeled with GPA-13 (E,F) or ODR-3 antibodies (G,H).